

Iterated Q -Network: Beyond One-Step Bellman Updates in Deep Reinforcement Learning

Théo Vincent^{1,2,*} Daniel Palenicek^{2,3} Boris Belousov¹

Jan Peters^{1,2,3,4} Carlo D'Eramo^{2,3,5}

¹DFKI GmbH, SAIROL ² Department of Computer Science, TU Darmstadt

³ Hesslan.ai ⁴ Centre for Cognitive Science, TU Darmstadt

⁵Center for Artificial Intelligence and Data Science, University of Würzburg

Abstract

The vast majority of Reinforcement Learning methods is largely impacted by the computation effort and data requirements needed to obtain effective estimates of action-value functions, which in turn determine the quality of the overall performance and the sample-efficiency of the learning procedure. Typically, action-value functions are estimated through an iterative scheme that alternates the application of an empirical approximation of the Bellman operator and a subsequent projection step onto a considered function space. It has been observed that this scheme can be potentially generalized to carry out multiple iterations of the Bellman operator at once, benefiting the underlying learning algorithm. However, till now, it has been challenging to effectively implement this idea, especially in high-dimensional problems. In this paper, we introduce *iterated Q -Network* (iQN), a novel principled approach that enables multiple consecutive Bellman updates by learning a tailored sequence of action-value functions where each serves as the target for the next. We show that iQN is theoretically grounded and that it can be seamlessly used in value-based and actor-critic methods. We empirically demonstrate the advantages of iQN in Atari 2600 games and MuJoCo continuous control problems.

1 Introduction

Deep Reinforcement Learning (RL) algorithms have achieved remarkable success in various fields, from nuclear physics (Degraeve et al., 2022) to construction assembly tasks (Funk et al., 2022). These algorithms aim at obtaining a good approximation of an action-value function through *consecutive* applications of the Bellman operator Γ to guide the learning procedure in the space of Q -functions, i.e., $Q_0 \rightarrow \Gamma Q_0 = Q_1 \rightarrow \Gamma Q_1 = Q_2 \rightarrow \dots$ (Bertsekas, 2019). This process is known as *value iteration*. *Approximate value iteration* (AVI) (Farahmand, 2011) extends the value iteration scheme to function approximation by adding a projection step, $Q_0 \rightarrow \Gamma Q_0 \approx Q_1 \rightarrow \Gamma Q_1 \approx Q_2 \rightarrow \dots$. Thus, the k^{th} Bellman update ΓQ_{k-1} gets projected back onto the chosen Q -function space via a new

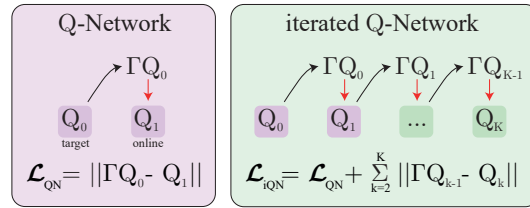


Figure 1: *Iterated Q -Network* (ours) uses the online network of regular Q -Network approaches to build a target for a second online network, and so on, through the application of the Bellman operator Γ . The resulting loss \mathcal{L}_{iQN} comprises K temporal difference errors instead of just one as in \mathcal{L}_{QN} .

*Correspondance to: theo.vincent@dfki.de

function Q_k approximating ΓQ_{k-1} . This projection step also appears in *approximate policy evaluation* (APE), where an empirical version of the Bellman operator for a behavioral policy is repeatedly applied to obtain its value function (Sutton & Barto, 1998).

In this paper, we discuss and tackle two efficiency issues resulting from the AVI learning scheme. **(i)** Projection steps are made sequentially, thus forcing to learn a Bellman update only at the end of the previous projection step, harming the efficiency of the training. **(ii)** Samples are only used to learn a *one-step* application of the Bellman operator at each gradient step, reducing sample-efficiency. We propose a novel approach to overcome these limitations by *learning consecutive Bellman updates simultaneously*. We leverage neural network function approximation to learn consecutive Bellman updates in a telescopic manner, forming a chain where each neural network learns the application of the Bellman operator over the previous one, as shown in Figure 1. This leads to a hierarchical ordering between the Q -estimates, where each one is the projection of the Bellman update corresponding to the previous one, hence the name *iterated Q-Network* (iQN). Importantly, iQN distributes the samples across all considered projection steps, thereby increasing the number of samples that each Q -function is learned from. Our approach can be seamlessly used in place of the regular one-step Bellman update by any value-based or actor-critic method, e.g., Deep Q -Network (DQN) (Mnih et al., 2015), Soft Actor-Critic (SAC) (Haarnoja et al., 2018). In the following, we motivate our approach theoretically and provide an algorithmic implementation that we validate empirically on Atari 2600 (Bellemare et al., 2013) and MuJoCo control problems (Todorov et al., 2012).

Contributions. (1) We introduce *iterated Q-Network* (iQN), a novel approach that enables learning multiple Bellman updates at once. (2) We provide intuitive and theoretical justifications for the advantages and soundness of iQN. (3) We show that iQN can be seamlessly combined with value-based and actor-critic methods to enhance their performance, conducting experiments on Atari games (Bellemare et al., 2013) and MuJoCo tasks (Todorov et al., 2012).

2 Preliminaries

We consider discounted Markov decision processes (MDPs) defined as $\mathcal{M} = \langle \mathcal{S}, \mathcal{A}, \mathcal{P}, \mathcal{R}, \gamma \rangle$, where \mathcal{S} and \mathcal{A} are measurable state and action spaces, $\mathcal{P} : \mathcal{S} \times \mathcal{A} \rightarrow \Delta(\mathcal{S})^2$ is a transition kernel, $\mathcal{R} : \mathcal{S} \times \mathcal{A} \rightarrow \mathbb{R}$ is a reward function, and $\gamma \in [0, 1)$ is a discount factor (Puterman, 1990). A policy is a function $\pi : \mathcal{S} \rightarrow \Delta(\mathcal{A})$, inducing an action-value function $Q^\pi(s, a) \triangleq \mathbb{E}_\pi [\sum_{t=0}^{\infty} \gamma^t \mathcal{R}(s_t, a_t) | s_0 = s, a_0 = a]$ that gives the expected discounted cumulative return executing action a in state s , following policy π thereafter. The objective is to find an optimal policy $\pi^* = \operatorname{argmax}_\pi V^\pi(\cdot)$, where $V^\pi(\cdot) = \mathbb{E}_{a \sim \pi(\cdot)} [Q^\pi(\cdot, a)]$. Approximate value iteration (AVI) and approximate policy iteration (API) are two common paradigms to tackle this problem (Sutton & Barto, 1998). While AVI aims to find the optimal action-value function $Q^*(\cdot, \cdot) \triangleq \max_\pi Q^\pi(\cdot, \cdot)$, API alternates between approximate policy evaluation (APE) to estimate the action-value function of the current policy and policy improvement that improves the current policy from the action-value function obtained from APE.

Both paradigms aim to find the fixed point of a Bellman equation by repeatedly applying a Bellman operator starting from a random Q -function. AVI uses the *optimal Bellman operator* Γ^* , whose fixed point is Q^* , while APE relies on the *Bellman operator* Γ^π associated with a policy π , whose fixed point is Q^π (Bertsekas, 2015). For any state $s \in \mathcal{S}$ and action $a \in \mathcal{A}$, Γ^* and Γ^π are defined as

$$(\Gamma^* Q)(s, a) \triangleq \mathbb{E}_{s' \sim \mathcal{P}(s, a)} [\mathcal{R}(s, a) + \gamma \max_{a' \in \mathcal{A}} Q(s', a')], \quad (1)$$

$$(\Gamma^\pi Q)(s, a) \triangleq \mathbb{E}_{s' \sim \mathcal{P}(s, a)} [\mathcal{R}(s, a) + \gamma \mathbb{E}_{a' \sim \pi(s')} Q(s', a')]. \quad (2)$$

It is well-known that these operators are contraction mappings in L_∞ -norm, such that their iterative application leads to their fixed point in the limit (Bertsekas, 2015). However, in model-free RL, only sample estimates of those operators are used since the expectations cannot be computed in closed form. This approximation, coupled with the use of function approximation to cope with large state-action spaces, forces learning the values of a Bellman update before being able to compute the next Bellman update. This procedure, informally known as *projection step*, results in a sequence of projected functions (Q_i) that does not correspond to the one obtained from the consecutive applications of the true Bellman operator, as shown in Figure 2a, where Γ equals Γ^* for AVI and Γ^π for APE. We

² $\Delta(\mathcal{X})$ denotes the set of probability measures over a set \mathcal{X} .

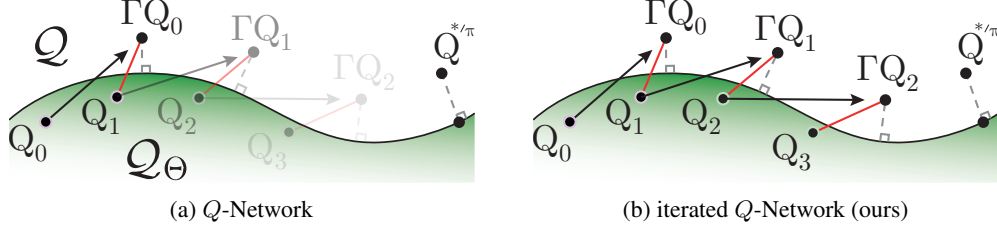


Figure 2: Graphical representation of the regular Q -Network approach (left) compared to our proposed iterated Q -Network approach (right) in the space of Q -functions \mathcal{Q} . The regular Q -Network approach proceeds sequentially, i.e., Q_2 is learned only when the learning process of Q_1 is finished. With iterated Q -Network, all parameters are learned simultaneously. The projection of $Q^{*/\pi}$ and projections of the Bellman update are depicted with a dashed line³. The losses are shown in red.

denote \mathcal{Q}_Θ as the space of function approximators, where Θ is the space of parameters. To learn a Bellman update $\Gamma Q_{\bar{\theta}_0}$ given a fixed parameter vector $\bar{\theta}_0 \in \Theta$, for a sample s, a, r, s' , Temporal Difference (TD) learning (Hasselt, 2010; Haarnoja et al., 2018) aims to minimize

$$\mathcal{L}_{\text{QN}}(\theta_1 | \bar{\theta}_0, s, a, r, s') = \left(\hat{\Gamma}_{r,s'} Q_{\bar{\theta}_0}(s, a) - Q_{\theta_1}(s, a) \right)^2, \quad (3)$$

over parameters $\theta_1 \in \Theta$, where $\hat{\Gamma}_{r,s'}$ is an empirical estimate of Γ and QN stands for Q -Network. In current approaches, a single Bellman update is learned at a time. The training starts by initializing the target parameters $\bar{\theta}_0$ and the online parameters θ_1 . The distance between Q_{θ_1} , representing the second Q -function Q_1 , and $\Gamma Q_{\bar{\theta}_0}$, representing the first Bellman update ΓQ_0 , is minimized via the loss in Equation 3, as shown in Figure 2a. After a predefined number of gradient steps, the procedure repeats, as in Figure 2a, where the second and third projection steps are blurred to stress the fact that they are learned sequentially. However, this sequential execution is computationally inefficient because it requires many non-parallelizable gradient steps to train a single projection. Moreover, this procedure is sample-inefficient since, at each gradient step, samples are used to learn only one Bellman update. In this work, we present a method that learns multiple Bellman updates at each gradient from a *single* sample batch. Importantly, our method scales to deep RL as shown in Section 6.

3 Related work

Several methods have been proposed on top of Q -learning to improve a variety of aspects. A large number of those algorithms focus on variants of the empirical Bellman operator (Van Hasselt et al., 2016; Fellows et al., 2021; Sutton, 1988). For instance, double DQN (Van Hasselt et al., 2016) uses an empirical Bellman operator designed to avoid overestimating the return. As shown in Figure 3, this results in a different location of the Bellman update $\tilde{\Gamma}Q$ compared to the classical Bellman update ΓQ . Likewise, n -step return (Watkins, 1989) considers another optimal Bellman operator, thus deriving another empirical Bellman operator. It computes the target as an interpolation between a one-step bootstrapping and a Monte-Carlo estimate. Other approaches consider changing the space of representable Q -functions \mathcal{Q}_Θ (Wang et al., 2016; Osband et al., 2016; Fatemi & Tavakoli, 2022; Ota et al., 2021; Bhatt et al., 2024), attempting to improve the projection of $Q^{*/\pi}$ on \mathcal{Q}_Θ compared to the one for the chosen baseline’s neural network architecture. It is important to note that adding a single neuron to one architecture layer can significantly change \mathcal{Q}_Θ . Wang et al. (2016) show that performance can be increased by including inductive bias into the neural network architecture. This idea can be understood as a modification of \mathcal{Q}_Θ , as shown in Figure 3 where the new space of representable Q -function $\tilde{\mathcal{Q}}_\Theta$ is colored in yellow. Furthermore, algorithms such as Rainbow (Hessel et al., 2018) leverage both ideas.

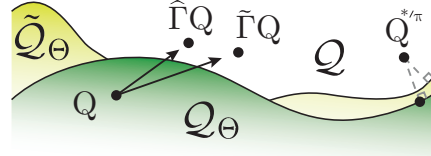


Figure 3: Other empirical Bellman operators can be represented using another notation $\tilde{\Gamma}$ than the classical empirical Bellman operator $\hat{\Gamma}$. Changing the class of function approximators \mathcal{Q}_Θ results in a new space $\tilde{\mathcal{Q}}_\Theta$.

³The existence of a projection on \mathcal{Q}_Θ depends only on the choice of the function approximator. Note that even if the projection does not exist, the presented abstraction is still valid.

To the best of our knowledge, only a few works consider learning multiple Bellman updates concurrently. Vincent et al. (2024) propose using a HyperNetwork (Ha et al., 2016) to approximate the Q -function parameters resulting from consecutive Bellman updates. While the idea of learning a HyperNetwork seems promising, one limitation is that it is challenging to scale to action-value functions with millions of parameters (Mnih et al., 2015). Similarly, Schmitt et al. (2022) provide a theoretical study about the learning of multiple Bellman updates concurrently. They consider an off-policy learning setting for linear function approximation and focus on low-dimensional problems. Crucially, their study shows that, in the limit, the concurrent learning of a sequence of consecutive Q -functions converges to the same sequence of Q -functions when learning is carried out sequentially. This finding leads to the following statement: *we do not need to wait until one Q -function has converged before learning the following one*. In this work, we pursue this idea by proposing a novel approach that scales with the number of parameters of the Q -function.

4 Learning multiple Bellman updates

We introduce our iterated Q -Network (iQN) approach to enable TD learning methods to carry out projections of consecutive Bellman updates simultaneously. For that, we consider K online networks parameterized by $(\theta_k)_{k=1}^K$, where θ_k is responsible for learning the k^{th} Bellman update, and K target networks $(\bar{\theta}_k)_{k=0}^{K-1}$, where each $\bar{\theta}_k$ is frequently updated to θ_k , for $k > 0$. Each θ_k learns from a target computed from $\bar{\theta}_{k-1}$. Thus, for each sample (s, a, r, s') , we propose to minimize

$$\mathcal{L}_{\text{iQN}}((\theta_k)_{k=1}^K | (\bar{\theta}_k)_{k=0}^{K-1}, s, a, r, s') = \frac{1}{K} \sum_{k=1}^K \mathcal{L}_{\text{QN}}(\theta_k | \bar{\theta}_{k-1}, s, a, r, s'), \quad (4)$$

where every D gradient steps the target networks are updated, $\bar{\theta}_k \leftarrow \theta_k$ for $k \in \{1, \dots, K-1\}$. The idea of iQN is to start learning the following projection steps parameterized by $(\theta_k)_{k=2}^K$ without waiting for θ_1 to be frozen. We highlight this idea by simultaneously showing three projection steps in Figure 2b, which visualizes a snapshot during the training when the target networks have been updated to the online networks. We complement this abstract visualization with Figure 12 in Appendix C.1, where we verify the described behavior in practice on a simple two-dimensional problem by applying our approach to Fitted- Q iteration (Ernst et al., 2005). After a fixed number of gradient steps T , the K pairs of online/target parameters are updated analogously to the way target updates are performed in DQN (Mnih et al., 2015) and SAC (Haarnoja et al., 2018). In the value-based setting, we shift forward the window of K Bellman updates, as shown in Figure 4. In detail, $\bar{\theta}_0 \leftarrow \theta_1$ and for $k \in \{1, \dots, K-1\}$, $\theta_k \leftarrow \theta_{k+1}$ and $\bar{\theta}_k \leftarrow \theta_k$. In the actor-critic setting, at each target update, we perform Polyak averaging (Lillicrap et al., 2015), i.e., we update the value of $\bar{\theta}_0$ to $\tau\theta_1 + (1-\tau)\bar{\theta}_0$, where $\tau \in [0, 1]$. The same is done for all the other θ_i with $i = 1, \dots, K-1$, so all the ΓQ_{θ_i} are also affected.

The availability of a sequence of approximations of consecutive Bellman updates raises the question of how to use them to draw actions. In regular Q -Network approaches, actions can only be drawn from the single online (or target) network. For iterated Q -Network approaches, one can choose which of the multiple online networks to sample from. We refer the reader to Section 6.1.1 where we investigate different sampling strategies.

iQN is an approach orthogonal to the choice of \mathcal{L}_{QN} ; thus, it can enable multiple simultaneous Bellman updates in any algorithm based on value function estimation. In the following, we consider the iterated versions of DQN (Mnih et al., 2015) and SAC (Haarnoja et al., 2018), namely *iterated Deep Q -Network* (iDQN) and *iterated Soft Actor-Critic* (iSAC), whose pseudocodes are shown in Appendix B. We point out that, when $K = 1$, the original algorithm is recovered.

5 Analysis of iterated Q -Network

To analyze our approach, we first note that the idea of learning consecutive Bellman iterations has been proposed by Schmitt et al. (2022), which prove that the concurrent update of chained Bellman

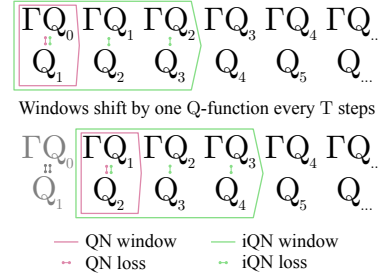


Figure 4: iQN considers a window of K Bellman updates as opposed to QN methods that consider only 1 Bellman updates. Every T gradient steps, the windows are shifted forward to consider the following Bellman updates.

updates converges to the same sequence of Q -functions that is found when the Q -functions are learned sequentially. In this section, we provide an analysis of iQN without assuming the use of linear function approximation. We support this analysis with an empirical evaluation on fitted Q -iteration (FQI) in the car-on-hill environment (Ernst et al., 2005) using *non-linear* function approximation (Riedmiller, 2005). Details about this experiment are in Appendix C.2.

A well-known result in AVI establishes an upper bound on the *performance loss* $\|Q^* - Q^{\pi_N}\|$, where π_N is the greedy policy of Q_N , i.e., the last Q -function learned during training (Theorem 3.4, Farahmand (2011)). The only term of this upper bound that is controlled by the training procedure is the *sum of approximation errors* $\sum_{k=1}^N \|\Gamma^* Q_{k-1} - Q_k\|_{2,\nu}^2$, where ν is the distribution of the state-action pairs in the replay buffer. As identified by Vincent et al. (2024), the theoretical benefit of learning multiple Bellman updates simultaneously is that a larger proportion of this sum is optimized compared to when the Bellman updates are learned sequentially. Leveraging this, iQN accounts for K approximation errors at each gradient step, differently from QN that only considers one term at a time. We observe this benefit in practice in a toy experiment on the car-on-hill environment, a simple variant of mountain-car described in Ernst et al. (2005). We set $N = 40$. As opposed to the way the windows are shifted in Figure 4, we shift the windows faster for lower values of K so that each algorithm has learned $N = 40$ Bellman updates at the end of the training. On the left axis of Figure 5, we show that for higher values of K , we obtain lower performance losses (in solid lines). If the training continues, the iterated approach keeps learning the last $K - 1$ projection steps since the considered windows would still contain those terms. In dashed lines, we show that continuing the training would further improve the performances. Moreover, on the right axis of Figure 5, we show that the sum of approximation errors decreases as K increases (where $K = 1$ corresponds to the regular QN approach). As expected, this is in accordance with the aforementioned theoretical results of Theorem 3.4 of Farahmand (2011) and Vincent et al. (2024). The effect of performing multiple Bellman updates is also evident from a visual interpretation of the plots, where one can see that increasing the value of K results in shrinking the plots obtained for smaller values of K . This is explained by the ability of iQN to look ahead of multiple Bellman iterations, thus anticipating the behavior of less far-sighted variants and speeding up learning. It is important to note that car-on-hill needs approximately 20 FQI iterations to be solved, for which reason iQN with $K = 20$ has an evident advantage over the other values of K .

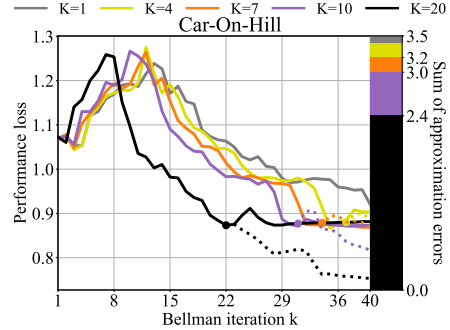


Figure 5: Distance between the optimal value function V^* and V^{π_k} at each iteration k for different K .

We can identify one caveat due to the fact that iQN is a semi-gradient method using target networks. Since the target networks are frozen, there is a gap between them and the corresponding online networks (see Figure 6). For clarity, we note $Q_k = Q_{\theta_k}$ and $\bar{Q}_k = Q_{\bar{\theta}_k}$. This means that a decrease in the loss of iQN does not necessarily correspond to a decrease of the sum of approximation errors $\|\Gamma^* \bar{Q}_0 - Q_1\|_{2,\nu}^2 + \sum_{k=2}^K \|\Gamma^* Q_{k-1} - Q_k\|_{2,\nu}^2$. This can be verified empirically, by showing that the percentage of times the considered sum of approximation errors does not decrease is higher for higher values of K , as shown on the first line of Table 1. Nonetheless, it appears that, on average, the

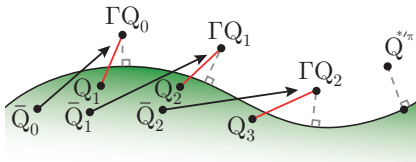


Figure 6: Graphical representation of iQN when each target networks \bar{Q}_k has not been updated to its respective online network Q_k .

K	1	4	7	10	20
% of the time the CSAE does not decrease	0	17	23	23	24
Average decrease of the CSAE ($\times 10^{-4}$)	0.3	1.5	2.6	3.9	7.8
% of the time Eq. 6 holds when Eq. 5 holds	100	100	100	100	100
% of the time Eq. 5 holds when Eq. 6 holds	100	17	17	17	17

Table 1: Empirical evaluation of the considered *sum of approximation errors* (CSAE) and Equations 5 and 6 on car-on-hill with iQN applied to FQI for different K .

considered sum of approximation errors decreases when K increases, as the second line of Table 1 shows. This is coherent with the results shown in Figure 5, as the sum of approximation errors is lower for higher values of K . To quantify the frequency with which the sum of approximation errors is effectively minimized when using iQN, we derive a sufficient condition under which this property holds (proof in Appendix A).

Proposition 5.1. *For $t \in \mathbb{N}$, let $(\theta_k^t)_{k=0}^K$ be a sequence of parameters of Θ and ν be a probability distribution over state-action pairs. Let $t \in \mathbb{N}$, if, for every $k \in \{1, \dots, K\}$,*

$$\underbrace{\|\Gamma^* Q_{\theta_{k-1}^{t+1}} - \Gamma^* Q_{\theta_{k-1}^t}\|_{2,\nu}}_{\text{displacement of the target}} \leq \underbrace{\|\Gamma^* Q_{\theta_{k-1}^t} - Q_{\theta_k^t}\|_{2,\nu}}_{\text{approx error before optimization}} - \underbrace{\|\Gamma^* Q_{\theta_{k-1}^t} - Q_{\theta_k^{t+1}}\|_{2,\nu}}_{\text{is minimized by the } k^{\text{th}} \text{ term of the loss}} \quad (5)$$

then, we have

$$\underbrace{\sum_{k=1}^K \|\Gamma^* Q_{\theta_{k-1}^{t+1}} - Q_{\theta_k^{t+1}}\|_{2,\nu}^2}_{\text{sum of approx errors after optimization}} \leq \underbrace{\sum_{k=1}^K \|\Gamma^* Q_{\theta_{k-1}^t} - Q_{\theta_k^t}\|_{2,\nu}^2}_{\text{sum of approx errors before optimization}} \quad (6)$$

As explained in Section 4, every D gradient steps, we update the target parameters $\bar{\theta}_k$ to be equal to their respective online parameters θ_k . We note $(\theta_k^t)_{k=0}^K$ the value of the parameters the t^{th} time this update is made. By applying Proposition 5.1 to those parameters, we see that the condition in Equation 5 holds when, for every $k \in [1, \dots, K]$, the gain obtained by the k^{th} vector of parameters θ_k^{t+1} of $\|\Gamma^* Q_{\theta_{k-1}^t} - Q_{\theta_k^{t+1}}\|_{2,\nu}$ over its previous version $\|\Gamma^* Q_{\theta_{k-1}^t} - Q_{\theta_k^t}\|_{2,\nu}$ is greater than the displacement of the targets $\|\Gamma^* Q_{\theta_{k-1}^{t+1}} - \Gamma^* Q_{\theta_{k-1}^t}\|_{2,\nu}$. Under this condition, the considered sum of approximation errors is reduced. Empirically, we show on the third line of Table 1 that when the proposed condition is verified (Equation 5 holds), then the considered sum of approximation errors decreases (Equation 6 holds). Moreover, the last line of the table shows the frequency with which the proposed condition is verified (Equation 5 holds) when the sum of approximation errors decreases (Equation 6 holds). For the considered example, this condition can explain the decrease of the considered sum of approximation errors for 17% of the time. For $K = 1$, this metric is at 100%, which is expected since the proposed condition is equivalent to a decrease in the considered sum of approximation errors. Indeed, when $K = 1$, the displacement to the target is null since θ_0^t , the only target parameter, is constant in t .

5.1 Iterated Q -network vs. n -step return

We point out that iQN is not equivalent to n -step return. While our approach aims at learning multiple consecutive projection steps simultaneously, n -step return applies Bellman updates considering a sequence of n consecutive rewards and the bootstrapped target at the n^{th} step. We empirically show the difference between iQN and n -step return in Figure 7, where DQN with 5-step return behaves substantially worse than iDQN with $K = 5$ on 4 randomly selected Atari games. The individual training curves are shown in Figure 18 of Appendix E.

One parallel can be done to link the two approaches in the APE setting. Indeed, using n -step return can be seen as applying the empirical Bellman operator n times. With $n = 2$, $(\hat{\Gamma}^\pi)^2 Q(s, a) = r_0 + \gamma \hat{\Gamma}^\pi Q(s_1, \pi(s_1)) = r_0 + \gamma(r_1 + \gamma Q(s_2, \pi(s_2))) = r_0 + \gamma r_1 + \gamma^2 Q(s_2, \pi(s_2))$. Thus, combining the idea of learning K Bellman updates with n -step return artificially brings the length of the window to $n \times K$ where K consecutive projections of the Bellman operator applied n times are learned. This fact is also discussed in Section 5.3 of Schmitt et al. (2022). It is worth noticing that this is not the case for AVI since the max operator is not linear. With $n = 2$, $(\hat{\Gamma}^*)^2 Q(s, a) = r_0 + \gamma \max_{a_1} \hat{\Gamma}^* Q(s_1, a_1) = r_0 + \gamma \max_{a_1} (r_1 + \gamma \max_{a_2} Q(s_2, a_2)) \neq r_0 + \gamma r_1 + \gamma^2 \max_{a_2} Q(s_2, a_2)$. Nonetheless, n -step return can be seamlessly used in iQN, and we show that the iterated version of DQN + 3-step return outperforms its sequential counterpart (Figure 7).

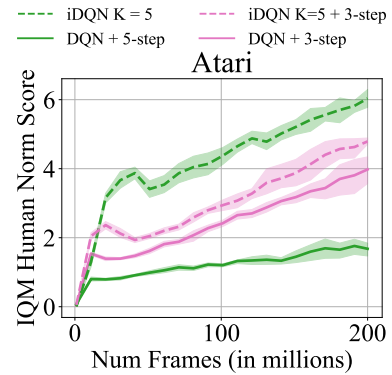


Figure 7: iDQN with $K = 5$ performs differently than DQN + 5-step return. DQN + 3-step return can be improved by learning 5 Bellman iterations at a time.

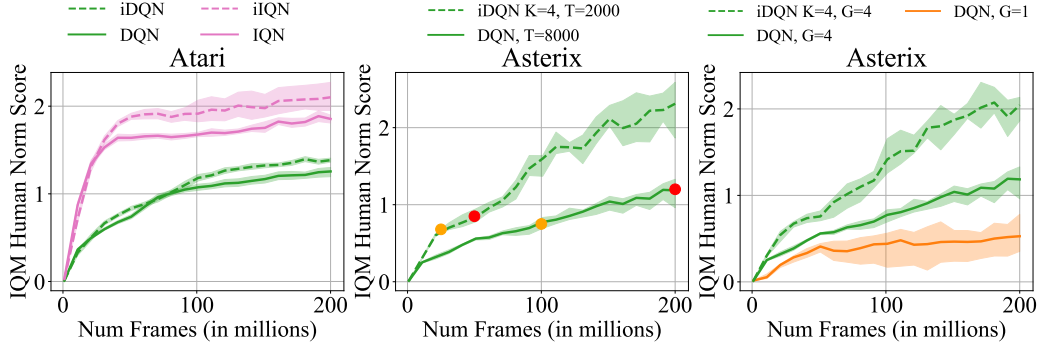


Figure 8: **Left:** iDQN and iQN outperform their respective sequential approach. **Middle:** iDQN with $K = 4, T = 2000$ parallelizes the training of DQN $T = 8000$ successfully since it yields similar performances after 3125 projection steps (in orange). This parallelization saves samples and gradient steps which can be used later to outperform DQN. **Right:** iDQN with $K = 4$ uses the sample 4 times more than DQN, both with $G = 4$. However, when DQN uses the samples as much as iDQN uses them ($G = 1$), it still performs worse than iDQN.

6 Experiments

We evaluate our proposed iQN approach on deep value-based and actor-critic settings. As recommended by Agarwal et al. (2021), we choose the interquartile mean (IQM) of the human normalized score to report the results of our experiments with shaded regions showing pointwise 95% percentile stratified bootstrap confidence intervals. IQM is a trade-off between the mean and the median where the tail of the score distribution is removed on both sides to consider only 50% of the runs. 5 seeds are used for each Atari game, and 10 seeds are used for each MuJoCo environment.

6.1 Atari 2600

We evaluate the iterated version of DQN and implicit quantile network (IQN) (Dabney et al., 2018) on 20 Atari 2600 games. Many implementations of Atari environments along with classical baselines are available (Castro et al., 2018; D’Eramo et al., 2021; Raffin et al., 2021; Huang et al., 2022). We choose to mimic the implementation choices made in Dopamine RL (Castro et al., 2018) since it is the only one to release the evaluation metric for the baselines that we consider and the only one to use the evaluation metric recommended by Machado et al. (2018). Namely, we use the *game over* signal to terminate an episode instead of the *life* signal. The input given to the neural network is a concatenation of 4 frames in grayscale of dimension 84 by 84. To get a new frame, we sample 4 frames from the Gym environment (Brockman et al., 2016) configured with no frame-skip, and we apply a max pooling operation on the 2 last grayscale frames. We use sticky actions to make the environment stochastic (with $p = 0.25$). The performance is the one obtained during training. By choosing an identical setting as Castro et al. (2018), we refer to the baselines’ training performance reported in Dopamine RL. To ensure that the comparison is fair, we compared our version of DQN and IQN to their version and verified their equivalence (see Figures 14 and 15 in Appendix C.3).

Hyperparameter settings. We use the same hyperparameters of the baselines, except for the target update frequency, which we set 25% lower than the target update frequency of the baselines (6000 compared to 8000). This is done because iQN carries out more gradient steps per projection step. We choose $D = 30$, and we let the Q -functions share the convolutional layers. We present the architecture of iQN in Figure 13 in Appendix C.3. Further details about the hyperparameters can be found in Table 2 in Appendix C.3. To ensure that our implementation is trustworthy, Figures 14 and 15 in Appendix C.3 show that the training performances of DQN and IQN are comparable to the ones of iDQN and iQN with $K = 1$, as expected.

Atari results. iDQN with $K = 5$ outperforms DQN on the aggregation metric, as shown in Figure 8 (left), both in terms of sample-efficiency and overall performance. In Figure 16 in Appendix E, the distribution of final scores illustrates that iDQN statistically dominates DQN on most of the scores. Notably, the iterated version of IQN with $K = 3$ greatly outperforms the sequential approach. All the individual training curves for the 20 Atari games are available in Figure 17 in Appendix E.

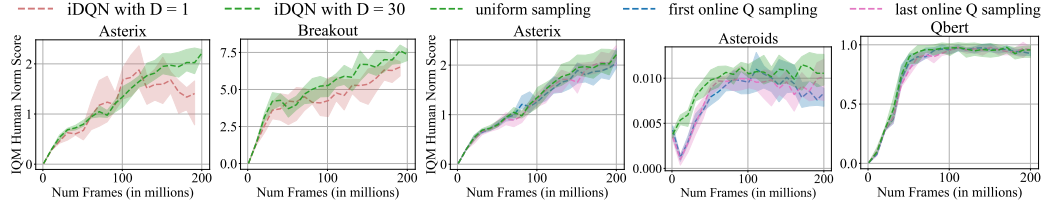


Figure 9: **Left:** Ablations on Asterix and Breakout indicate improved performance with delayed parameters. **Right:** Ablation study on the way actions are sampled to interact with the environment.

6.1.1 Ablation studies

On top of the ablation studies that we conduct in the following paragraphs, Appendix E contains 3 additional ablation studies about the choice of sharing the convolutional layers, the hyperparameter K , and the variability of the networks during training.

Learning projection steps simultaneously. In Section 5, we provide a condition under which the loss of iQN minimizes the sum of approximation errors, thus establishing when starting to learn the following projection steps is beneficial. In Figure 8 (middle), we set the target update frequency to be a fourth of the one of DQN (2000 instead of 8000). Since $K = 4$, each projection step is learned on the same number of samples. We mark in orange the performance after 3125 ($100 \times 250000/8000 = 25 \times 250000/2000 = 3125$) projection steps and in red the performance after 6250 projection steps. Interestingly, the performances of iDQN and DQN after 3125 projection steps are similar, showing that waiting for one projection step to finish to do the next one is not necessary. After 6250 projection steps, the performances of iDQN are slightly below the ones of DQN. We believe that this comes from the fact that, at this point of the training, DQN has 4 times more environment interactions than iDQN. Nevertheless, by learning the 3 following projection steps while the first one is being learned, iDQN is more efficient than DQN.

Sharing samples across multiple projection steps. A major advantage of iQN is the ability to share samples across consecutive projection steps. In Figure 8 (right), we set $K = 4$ and the target update frequency of iDQN to be the *same* as DQN, i.e., 8000. This way, the only difference between iDQN and DQN ($G = 4$) is that each projection step of iDQN is learned on 4 times more samples than DQN ($G = 4$). G is the number of samples collected between each gradient step, set to 4 in DQN. One can see that this difference brings a significant advantage to iDQN. The loss of iQN presented in Equation 4 is composed of the sum of TD-errors. This means that iQN implicitly does more gradient steps than the sequential approach. However, we argue the number of non-parallelizable gradient steps is more important than the implicit number of gradient steps since enough parallel processing power can make parallelizable gradient steps as fast as one gradient step. Nevertheless, we evaluate a version of DQN having the same number of implicit gradient steps per projection step as iDQN, i.e., we set $G = 1$. This variation leads to overfitting while having a training time 89% longer than iDQN.

Decreasing the frequency at which the target networks are updated. Figure 9 (left) shows the performance of iDQN with $D = 1$, i.e., the target networks are updated to their respective online networks at every gradient step and with $D = 30$ on 2 Atari games. iDQN with $D = 1$ obtains worse results and even drops performance on *Asterix*.

Uniform sampling across Q -functions for action selection. As explained in Section 4, the availability of several online Q -functions corresponding to K consecutive Bellman updates raises the question of which network to use for the behavioral policy. Informally, we can argue that along the chain of Q -functions in iDQN, on the one hand, the first network is the one with the best estimate of its respective Bellman update, but the most distant from the optimal Q -function. On the other hand, the last network is the less accurate, but the most far-sighted one. This creates a trade-off between accuracy and distance from the optimal Q -function, that we face by sampling a network uniformly at each step. We compare the performance of our uniform sampling strategy and the use of the first and last network, showing a slight superiority of uniform sampling (Figure 9 (right)). We postpone the study of more principled sampling strategies to future works.

Comparing different window sizes. As shown in Figure 10, increasing K from 5 to 10 iterations is beneficial for the games *Asteroids* and *Asterix*. However, the difference between $K = 5$ and $K = 10$

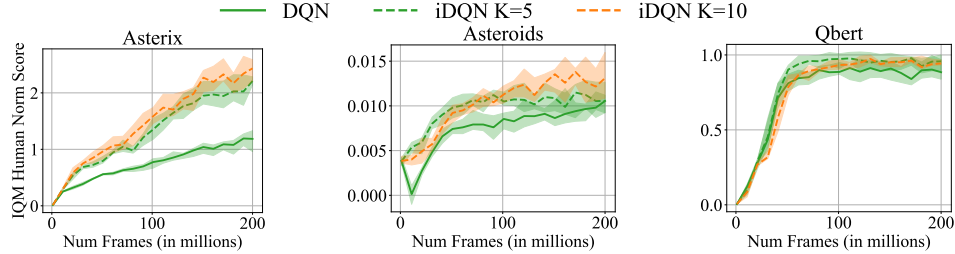


Figure 10: Ablation study on the number of Bellman updates K taken into account in the loss. Greater performances are reached for greater values of K in *Asteroids* and *Asterix*. In *Qbert*, iDQN with $K = 10$ might allow the agent to overfit the targets since each Bellman update is learned with 10 times more gradient steps. We recall that DQN is equivalent to iDQN with $K = 1$.

is mild. This suggests that even small window sizes can have a big impact on performance, which is desirable for efficiency. Because of this, we choose $K = 5$ for most of our Atari experiments.

6.2 MuJoCo continuous control

We evaluate our proposed iterated approach over two actor-critic algorithms on 6 different MuJoCo environments. We build iSAC on top of SAC and iDroQ on top of DroQ (Hiraoka et al., 2022). We set $K = 4$, meaning that the iterated versions consider 4 Bellman updates in the loss instead of 1. Therefore, we set the soft target update rate τ to 4 times higher than the sequential baseline algorithms (0.02 compared to 0.005) while keeping all other hyperparameters identical. Figure 11 shows the training performances of iSAC and iDroQ against their respective baselines. The IQM return is normalized by the final performance of SAC. Both iterated versions outperform their respective sequential counterparts. While iDroQ dominates DroQ until the end of the training at 1 million environment interactions, iSAC finally converges to the same performances as SAC. Per environment plots are available in Figure 23 of Appendix F. In Figures 22 and 24 of Appendix F, we show the performances of SAC and DroQ with the same soft target update rate τ as iSAC and iDroQ. The iterated approaches still outperform the sequential approaches, showing that learning multiple Bellman updates in parallel is beneficial. Table 4 in Appendix C.4 gathers all the hyperparameters used in this section.

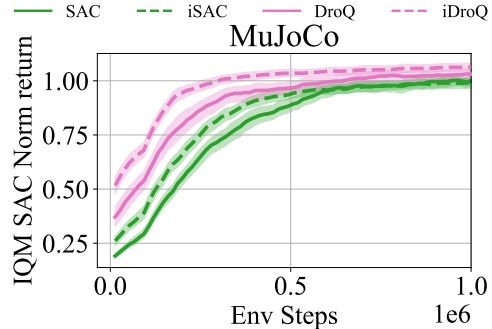


Figure 11: Training curves of iSAC and iDroQ ($K = 4$) along with SAC and DroQ. The iterated versions significantly outperform their sequential counterparts. The curves are normalized by the final performance of SAC.

7 Discussion and conclusion

We have presented iterated Q -Network (iQN), a new approach that considers multiple consecutive projection steps in the loss to overcome the limitations of the one-step Bellman updates. We have theoretically and empirically analysed its benefit across several problems when applied to deep value-based algorithms and actor-critic methods. One limitation of iQN is the required training time compared to the sequential approach for the same number of gradient steps, as shown in the first line of Table 5 in Appendix D. Potentially, this becomes similar to the one of a regular Q -Network, if enough parallel processing power is available. Nevertheless, by performing better than the baselines, as the second line of Table 5 shows, iQN reaches the final performances of QN faster, as the third line of the table indicates. Another limitation is the higher memory requirements of iQN, compared to QN, due to the need to keep multiple online/target networks loaded on the GPU (see the last line of Table 5). Notably, Figure 21 in Appendix E certifies that increasing the number of parameters of DQN to match the memory needed to run iDQN is underperforming compared to iDQN.

References

- Agarwal, R., Schuurmans, D., and Norouzi, M. An optimistic perspective on offline reinforcement learning. In *International conference on machine learning*, 2020.
- Agarwal, R., Schwarzer, M., Castro, P. S., Courville, A. C., and Bellemare, M. Deep reinforcement learning at the edge of the statistical precipice. In *Advances in neural information processing systems*, 2021.
- Bellemare, M. G., Naddaf, Y., Veness, J., and Bowling, M. The arcade learning environment: An evaluation platform for general agents. *Journal of artificial intelligence research*, 47:253–279, 2013.
- Bertsekas, D. *Reinforcement learning and optimal control*. Athena Scientific, 2019.
- Bertsekas, D. P. *Dynamic programming and optimal control 4th edition, volume II*. Athena scientific, 2015.
- Bhatt, A., Palenicek, D., Belousov, B., Argus, M., Amiranashvili, A., Brox, T., and Peters, J. Crossq: Batch normalization in deep reinforcement learning for greater sample efficiency and simplicity. In *International conference on learning representations*, 2024.
- Bradbury, J., Frostig, R., Hawkins, P., Johnson, M. J., Leary, C., Maclaurin, D., Necula, G., Paszke, A., VanderPlas, J., Wanderman-Milne, S., and Zhang, Q. JAX: composable transformations of Python+NumPy programs, 2018.
- Bradtke, S. Reinforcement learning applied to linear quadratic regulation. In *Advances in neural information processing systems*, 1992.
- Brockman, G., Cheung, V., Pettersson, L., Schneider, J., Schulman, J., Tang, J., and Zaremba, W. Openai gym, 2016.
- Castro, P. S., Moitra, S., Gelada, C., Kumar, S., and Bellemare, M. G. Dopamine: A research framework for deep reinforcement learning. *arXiv preprint arXiv:1812.06110*, 2018.
- Dabney, W., Ostrovski, G., Silver, D., and Munos, R. Implicit quantile networks for distributional reinforcement learning. In *International conference on machine learning*, 2018.
- Degrave, J., Felici, F., Buchli, J., Neunert, M., Tracey, B., Carpanese, F., Ewalds, T., Hafner, R., Abdolmaleki, A., de Las Casas, D., et al. Magnetic control of tokamak plasmas through deep reinforcement learning. *Nature*, 602(7897):414–419, 2022.
- D’Eramo, C., Tateo, D., Bonarini, A., Restelli, M., and Peters, J. Mushroomrl: Simplifying reinforcement learning research. *Journal of machine learning research*, 22(131):1–5, 2021.
- Ernst, D., Geurts, P., and Wehenkel, L. Tree-based batch mode reinforcement learning. *Journal of machine learning research*, 6(2005):503–556, 2005.
- Farahmand, A.-m. Regularization in reinforcement learning. 2011.
- Fatemi, M. and Tavakoli, A. Orchestrated value mapping for reinforcement learning. *arXiv preprint arXiv:2203.07171*, 2022.
- Fellows, M., Hartikainen, K., and Whiteson, S. Bayesian bellman operators. In *Advances in neural information processing systems*, 2021.
- Funk, N., Chalvatzaki, G., Belousov, B., and Peters, J. Learn2assemble with structured representations and search for robotic architectural construction. In *Conference on robot learning*, 2022.
- Ha, D., Dai, A., and Le, Q. Hypernetworks. In *International conference on learning representations*, 2016.
- Haarnoja, T., Zhou, A., Abbeel, P., and Levine, S. Soft actor-critic: Off-policy maximum entropy deep reinforcement learning with a stochastic actor. In *International conference on machine learning*, 2018.

- Hasselt, H. Double q-learning. In *Advances in neural information processing systems*, 2010.
- Hessel, M., Modayil, J., Van Hasselt, H., Schaul, T., Ostrovski, G., Dabney, W., Horgan, D., Piot, B., Azar, M., and Silver, D. Rainbow: Combining improvements in deep reinforcement learning. In *AAAI conference on artificial intelligence*, 2018.
- Hiraoka, T., Imagawa, T., Hashimoto, T., Onishi, T., and Tsuruoka, Y. Dropout q -functions for doubly efficient reinforcement learning. In *International conference on learning representations*, 2022.
- Huang, S., Dossa, R. F. J., Ye, C., Braga, J., Chakraborty, D., Mehta, K., and Araújo, J. G. Cleanrl: High-quality single-file implementations of deep reinforcement learning algorithms. *Journal of machine learning research*, 23(274):1–18, 2022.
- Kingma, D. P. and Ba, J. Adam: A method for stochastic optimization. In *International conference on learning representations*, 2015.
- Lillicrap, T. P., Hunt, J. J., Pritzel, A., Heess, N., Erez, T., Tassa, Y., Silver, D., and Wierstra, D. Continuous control with deep reinforcement learning. *arXiv preprint arXiv:1509.02971*, 2015.
- Machado, M. C., Bellemare, M. G., Talvitie, E., Veness, J., Hausknecht, M., and Bowling, M. Revisiting the arcade learning environment: Evaluation protocols and open problems for general agents. *Journal of artificial intelligence research*, 61:523–562, 2018.
- Mnih, V., Kavukcuoglu, K., Silver, D., Rusu, A. A., Veness, J., Bellemare, M. G., Graves, A., Riedmiller, M., Fidjeland, A. K., Ostrovski, G., et al. Human-level control through deep reinforcement learning. *Nature*, 518(7540):529–533, 2015.
- Osband, I., Blundell, C., Pritzel, A., and Van Roy, B. Deep exploration via bootstrapped dqn. In *Advances in neural information processing systems*, 2016.
- Ota, K., Jha, D. K., and Kanazaki, A. Training larger networks for deep reinforcement learning. *arXiv preprint arXiv:2102.07920*, 2021.
- Puterman, M. L. Markov decision processes. *Handbooks in operations research and management science*, 2:331–434, 1990.
- Raffin, A., Hill, A., Gleave, A., Kanervisto, A., Ernestus, M., and Dormann, N. Stable-baselines3: Reliable reinforcement learning implementations. *Journal of machine learning research*, 22(268):1–8, 2021.
- Riedmiller, M. Neural fitted q iteration—first experiences with a data efficient neural reinforcement learning method. In *European conference on machine learning*, pp. 317–328. Springer, 2005.
- Schmitt, S., Shawe-Taylor, J., and Van Hasselt, H. Chaining value functions for off-policy learning. In *AAAI conference on artificial intelligence*, 2022.
- Sutton, R. S. Learning to predict by the methods of temporal differences. *Machine learning*, 3(1):9–44, 1988.
- Sutton, R. S. and Barto, A. G. *Reinforcement learning: An introduction*. MIT Press, 1998.
- Todorov, E., Erez, T., and Tassa, Y. Mujoco: A physics engine for model-based control. In *International conference on intelligent robots and systems*, 2012.
- Van Hasselt, H., Guez, A., and Silver, D. Deep reinforcement learning with double q-learning. In *AAAI conference on artificial intelligence*, 2016.
- Vincent, T., Metelli, A., Belousov, B., Peters, J., Restelli, M., and D’Eramo, C. Parameterized projected bellman operator. In *AAAI conference on artificial intelligence*, 2024.
- Wang, Z., Schaul, T., Hessel, M., Hasselt, H., Lanctot, M., and Freitas, N. Dueling network architectures for deep reinforcement learning. In *International conference on machine learning*, 2016.
- Watkins, C. J. C. H. *Learning from Delayed Rewards*. PhD thesis, King’s College, Oxford, 1989.

A Proof of Proposition 5.1

Proposition A.1. For $t \in \mathbb{N}$, $(\theta_k^t)_{k=0}^K$ be a sequence of parameters of Θ and ν be a probability distribution over state-action pairs. Let $t \in \mathbb{N}$, if, for every $k \in \{1, \dots, K\}$,

$$\|\Gamma^* Q_{\theta_{k-1}^{t+1}} - \Gamma^* Q_{\theta_{k-1}^t}\|_{2,\nu} \leq \|\Gamma^* Q_{\theta_{k-1}^t} - Q_{\theta_k^t}\|_{2,\nu} - \|\Gamma^* Q_{\theta_{k-1}^t} - Q_{\theta_k^{t+1}}\|_{2,\nu} \quad (7)$$

then, we have

$$\sum_{k=1}^K \|\Gamma^* Q_{\theta_{k-1}^{t+1}} - Q_{\theta_k^{t+1}}\|_{2,\nu}^2 \leq \sum_{k=1}^K \|\Gamma^* Q_{\theta_{k-1}^t} - Q_{\theta_k^t}\|_{2,\nu}^2 \quad (8)$$

Proof. For $t \in \mathbb{N}$, let $(\theta_k^t)_{k=0}^K$ be a sequence of parameters of Θ and ν be a probability distribution over state-action pairs. Let $t \in \mathbb{N}$, we assume that for every $k \in \{1, \dots, K\}$ condition Equation 7 holds.

Now, we show that for every $k \in \{1, \dots, K\}$, $\|\Gamma^* Q_{\theta_{k-1}^{t+1}} - Q_{\theta_k^{t+1}}\|_{2,\nu} \leq \|\Gamma^* Q_{\theta_{k-1}^t} - Q_{\theta_k^t}\|_{2,\nu}$. From there, Equation 8 can be obtained by applying the square function to both sides of the inequality and by summing over k .

Let $k \in \{1, \dots, K\}$. To show that $\|\Gamma^* Q_{\theta_{k-1}^{t+1}} - Q_{\theta_k^{t+1}}\|_{2,\nu} \leq \|\Gamma^* Q_{\theta_{k-1}^t} - Q_{\theta_k^t}\|_{2,\nu}$, we start with the left side of the inequality

$$\begin{aligned} \|\Gamma^* Q_{\theta_{k-1}^{t+1}} - Q_{\theta_k^{t+1}}\|_{2,\nu} &= \|\Gamma^* Q_{\theta_{k-1}^{t+1}} - \Gamma^* Q_{\theta_{k-1}^t} + \Gamma^* Q_{\theta_{k-1}^t} - Q_{\theta_k^{t+1}}\|_{2,\nu} \\ &\leq \|\Gamma^* Q_{\theta_{k-1}^{t+1}} - \Gamma^* Q_{\theta_{k-1}^t}\|_{2,\nu} + \|\Gamma^* Q_{\theta_{k-1}^t} - Q_{\theta_k^{t+1}}\|_{2,\nu} \\ &\leq \|\Gamma^* Q_{\theta_{k-1}^t} - Q_{\theta_k^t}\|_{2,\nu}^2, \end{aligned}$$

The second last inequation comes from the triangular inequality, and the last inequation comes from the assumption that Equation 7 holds. \square

B Pseudocodes

Algorithm 1 Iterated Deep Q-Network (iDQN). Modifications to DQN are marked in purple.

- 1: Initialize the first target network $\bar{\theta}_0$ and the K online parameters $(\theta_k)_{k=1}^K$, and an empty replay buffer \mathcal{D} . For $k = 1, \dots, K - 1$, set $\bar{\theta}_k \leftarrow \theta_k$ the rest of the target parameters.
- 2: **repeat**
- 3: Sample $k^b \sim U\{1, \dots, K\}$.
- 4: Take action $a_t \sim \epsilon$ -greedy($Q_{\theta_{k^b}}(s_t, \cdot)$); Observe reward r_t , next state s_{t+1} .
- 5: Update $\mathcal{D} \leftarrow \mathcal{D} \cup \{(s_t, a_t, r_t, s_{t+1})\}$.
- 6: **every G steps**
- 7: Sample a mini-batch $\mathcal{B} = \{(s, a, r, s')\}$ from \mathcal{D} .
- 8: Compute the loss

$$\mathcal{L}_{\text{iDQN}} = \sum_{(s,a,r,s') \in \mathcal{B}} \sum_{k=1}^K \left(r + \gamma \max_{a'} Q_{\bar{\theta}_{k-1}}(s', a') - Q_{\theta_k}(s, a) \right)^2.$$

- 9: Update the online parameters θ_k from $\nabla_{\theta_k} \mathcal{L}_{\text{iDQN}}$, for $k \in \{1, \dots, K\}$.
 - 10: **every D steps**
 - 11: Update the target parameters $\bar{\theta}_k \leftarrow \theta_k$, for $k \in \{1, \dots, K - 1\}$.
 - 12: **every T steps**
 - 13: Shift the parameters $\bar{\theta}_0 \leftarrow \theta_1$ and $\bar{\theta}_k \leftarrow \theta_{k+1}$, for $k \in \{0, \dots, K - 1\}$.
 - 14: Update the target parameters $\bar{\theta}_k \leftarrow \theta_k$, for $k \in \{1, \dots, K - 1\}$.
-

Algorithm 2 Iterated Soft Actor-Critic (iSAC). Modifications to SAC are marked in purple.

- 1: Initialize the policy parameters ϕ , $2 \times K$ online parameters $((\theta_k^1, \theta_k^2))_{k=1}^K$, 2 target parameters θ_0^1, θ_0^2 , and an empty replay buffer \mathcal{D} .
- 2: **repeat**
- 3: Take action $a_t \sim \pi_\phi(\cdot|s_t)$; Observe reward r_t , next state s_{t+1} ; $\mathcal{D} \leftarrow \mathcal{D} \cup \{(s_t, a_t, r_t, s_{t+1})\}$.
- 4: **for** UTD updates **do**
- 5: Sample a mini-batch $\mathcal{B} = \{(s, a, r, s')\}$ from \mathcal{D} .
- 6: Compute the loss

$$\mathcal{L}_{\text{iSAC}} = \sum_{(s,a,r,s') \in \mathcal{B}} \sum_{k=1}^K \sum_{i=1}^2 \left(r + \gamma \left(\min_{j \in \{1,2\}} Q_{\theta_{k-1}^j}(s', a') - \alpha \log \pi_\phi(a'|s') \right) - Q_{\theta_k^i} \right)^2,$$

where $a' \sim \pi_\phi(\cdot|s')$.

- 7: Update θ_k^i from $\nabla_{\theta_k^i} \mathcal{L}_{\text{iQN}}$, for $i \in \{1, 2\}$ and $k \in \{1, \dots, K\}$.
- 8: Update the target networks $\theta_0^i \leftarrow \tau \theta_1^i + (1 - \tau) \theta_0^i$, for $i \in \{1, 2\}$.
- 9: Sample $k^b \sim U\{1, \dots, K\}$.
- 10: Update ϕ with gradient ascent using the loss

$$\min_{i \in \{1,2\}} Q_{\theta_{k^b}^i}(s, a) - \alpha \log \pi_\phi(a|s), \text{ where } a \sim \pi_\phi(\cdot|s).$$

C Experiments details

We used the optimizer Adam (Kingma & Ba, 2015) for all experiments. We used JAX (Bradbury et al., 2018) as a deep learning framework. **We provide the source code in the supplementary material and will publish it on github.com upon acceptance.**

C.1 Behavior of Q -network and iterated Q -network on a Linear Quadratic Regulator

Figures 2a, 2b are schematically representing the behavior of QN and iQN approaches in the space of Q -functions. Figure 12 shows that those representations are accurate for an offline problem: Linear Quadratic Regulator (Bradtke, 1992). In this problem, the state and action spaces are continuous and one-dimensional. The dynamics are linear: for a state s and an action a , the next state is given by $s' = 0.8s - 0.9a$, and the reward is quadratic $r(s, a) = 0.5s^2 + 0.4sa - 0.5a^2$. We choose to parametrize the space of Q -functions with 2 parameters (M, G) such that, for a state s and an action a , $Q(s, a) = Ma^2 + Gs^2$. To reduce the space of representable Q -functions, we constrain the parameter M to be negative and the parameter G to be between -0.4 and 0.4 . Starting from some initial parameters, we perform 30 gradient steps with a learning rate of 0.05 using the loss of QN and iQN. Both figures show the space of representable Q -functions \mathcal{Q}_Θ in green, the optimal Q -function Q^* , the initial Q -function Q_0 and its optimal Bellman update $\Gamma^* Q_0$. The projection of the optimal Bellman update is also shown with a dotted line. As we claim in the main paper, iQN manages to find a Q -function Q_2 closer to the optimal Q -function Q^* than Q_1 found by QN. Figure 12a closely resembles Figure 2a. Likewise, Figure 12b looks like Figure 2b, showing that the high-level ideas presented in the paper are actually happening in practice.

C.2 Experiments on the car-on-hill environment

Experimental setting. The dataset contains 50,000 samples collected with a uniform policy from the initial state $[-0.5, 0]$. We use a neural network with one hidden layer of 50 neurons. The batch size is 100 and we set $D = 1$. Each iFQI run has access to 20,000 gradient steps. The results are average over 20 seeds. In Figure 5, we report the performance loss $\|Q^* - Q^{\pi_N}\|_{\rho,1}$, where Q^{π_N} is the action-value function associated with the greedy policy of Q_N , which can be associated with the last network learned during training. ρ is usually associated to the state-action distribution on which we would like the chosen policy to perform well. Therefore, we choose ρ as a uniform distribution over the state space and action space on a 17×17 grid as suggested by Ernst et al. (2005). In Figure 5,

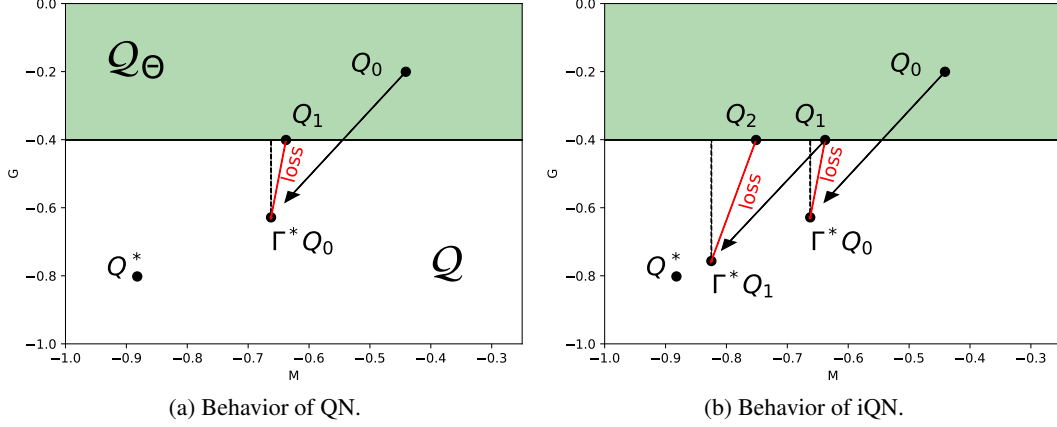


Figure 12: Graphical representation of QN (left) and iQN (right) in the space of Q -functions \mathcal{Q} for the LQR experiment.

we compute the sum of approximation errors $\sum_{k=1}^{40} \|\Gamma^* Q_{k-1} - Q_k\|_{\nu,2}^2$, where ν is the state-action distribution encountered during training, i.e., the data stored in the replay buffer.

C.3 Experiments on the Atari games

Table 2: Summary of all hyperparameters used for the Atari experiments. $\text{Conv}_{a,b}^d C$ is a 2D convolutional layer with C filters of size $a \times b$ and of stride d , and FCE is a fully connected layer with E neurons.

Environment	
Discount factor γ	0.99
Horizon H	27 000
Full action space	No
Reward clipping	$\text{clip}(-1, 1)$
All algorithms	
Number of epochs	200
Number of training steps per epochs	250 000
Type of the replay buffer \mathcal{D}	FIFO
Initial number of samples in \mathcal{D}	20 000
Maximum number of samples in \mathcal{D}	1 000 000
Gradient step frequency G	4
Starting ϵ	1
Ending ϵ	10^{-2}
ϵ linear decay duration	250 000
Batch size	32
Learning rate	6.25×10^{-5}
Adam ϵ	1.5×10^{-4}
Torso architecture	$\text{Conv}_{8,8}^4 32 - \text{Conv}_{4,4}^2 64 - \text{Conv}_{3,3}^1 64 -$
Head architecture	$- \text{FC}_{512} - \text{FC}_{n_A}$
Activations	ReLU
DQN & IQN	
Target step frequency T	8 000
iDQN & iIQN	
Target update frequency T	6 000
D	30

Atari game selection. The Atari benchmark is a highly compute-intensive benchmark. Depending on the hardware and the codebase, one seed for one Atari game can take between 1 day to 3 days to run DQN on a GPU. This is why we could not afford to run the experiments on the 57 games with 5 seeds. The 20 games were chosen before doing the experiments and never changed afterward. They were chosen such that the baselines and Rainbow have almost the same aggregated final scores for the 20 chosen games as the aggregated final scores shared by Dopamine RL as shown in Table 3.

Table 3: The IQM Human normalized final scores of the baselines and Rainbow aggregated over the 55 available Atari games are similar to the ones aggregated over the 20 chosen games.

	DQN	Rainbow	IQN
Final score over the 55 Atari games available in Dopamine RL	1.29	1.71	1.76
Final score over the 20 chosen Atari games	1.29	1.72	1.85

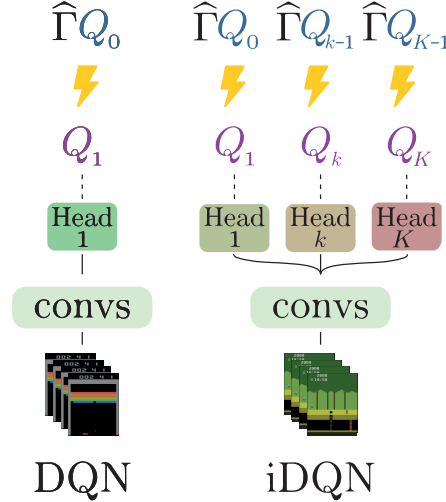


Figure 13: Losses and neural networks architectures of DQN and iDQN. The dotted lines link the outputs of the neural networks to the objects they represent. The flash signs stress how each projection step is being learned, where $\hat{\Gamma}$ is the empirical Bellman operator. The target networks are represented in blue while the online networks are in purple. For iQIN, the convolution layers of Q_0 are stored separately since it is the only target Q -function that is not updated every D gradient steps.

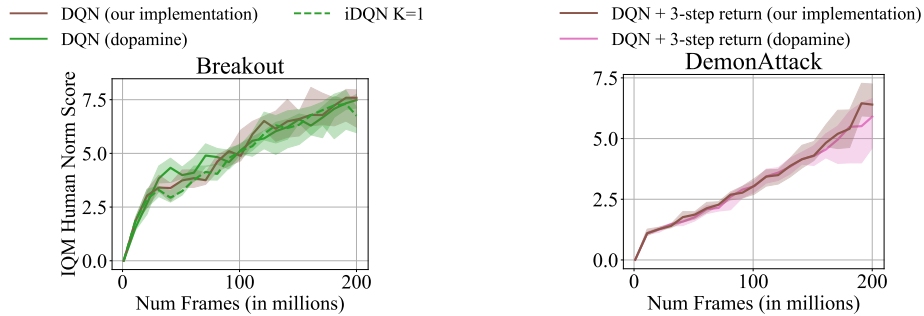


Figure 14: **Left:** Our implementation of DQN yields similar performance as the implementation of Dopamine RL. This certifies that we can compare the results released in Dopamine RL with our method. DQN and iDQN with $K = 1$ have a similar behavior. This certifies the trustworthiness of our code base. **Right:** We draw similar conclusions when adding a 3-step return.

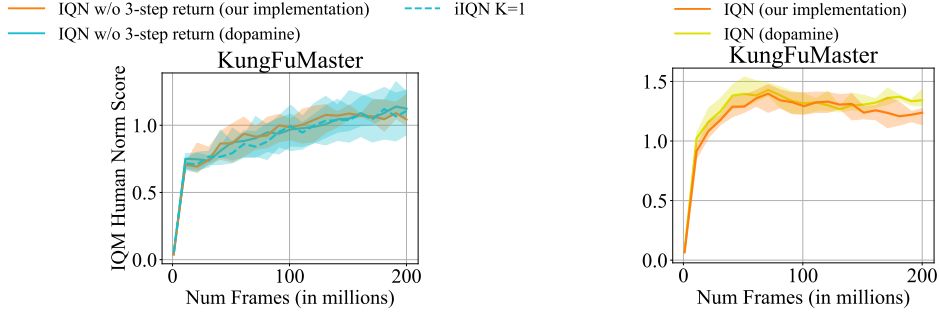


Figure 15: **Left:** Our implementation of IQN yields similar performance as the implementation of Dopamine RL. This certifies that we can compare the results released in Dopamine RL with our method. IQN and iQN with $K = 1$ have a similar behavior. This certifies the trustworthiness of our code base. **Right:** We draw similar conclusions when adding a 3-step return.

C.4 Experiments on the Mujoco control problems

Table 4: Summary of all hyperparameters used for the MuJoCo experiments.

Environment	
Discount factor γ	0.99
All algorithms	
Number of training steps	1 000 000
Type of the replay buffer \mathcal{D}	FIFO
Initial number of samples in \mathcal{D}	5 000
Maximum number of samples in \mathcal{D}	1 000 000
Update-To-Date UTD	1
Batch size	256
Learning rate	10^{-3}
Adam β_1	0.9
SAC & DroQ	
Soft target update frequency τ	5×10^{-3}
iSAC & iDroQ	
Soft target update frequency τ	2×10^{-2}
D	1

D Training time and memory requirements

Table 5: Final performances, memory requirements, and training time of iQN compared to QN. Computations are made on an NVIDIA GeForce RTX 4090 Ti. For iDQN and iQN, the game *Breakout* is used to compute the training time. For iSAC and iDroQ, the training time is averaged over the 6 considered environment.

	iDQN vs DQN for $K = 5$	iQN vs IQN for $K = 3$	iSAC vs SAC for $K = 4$	iDroQ vs DroQ for $K = 4$
Additional training time	31%	52%	10%	22%
Improvement in final performance	+10%	+13%	-1%	+3%
Time saved to reach QN's final performance	7h31m	18h23m	6m	1h55m
Additional GPU vRAM usage	0.3 Gb	0.9 Gb	0.1 Gb	0.4 Gb

E Training curves for Atari games

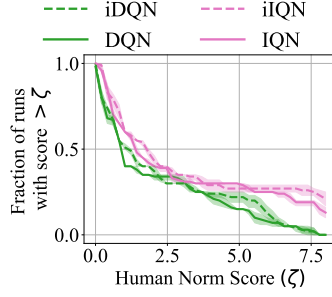


Figure 16: Performance profile. The figure shows the fraction of runs with a higher final score than a certain threshold given by the x -axis. The iterated versions, iDQN and iIQN, statistically dominate their respective sequential approach on most of the domain.

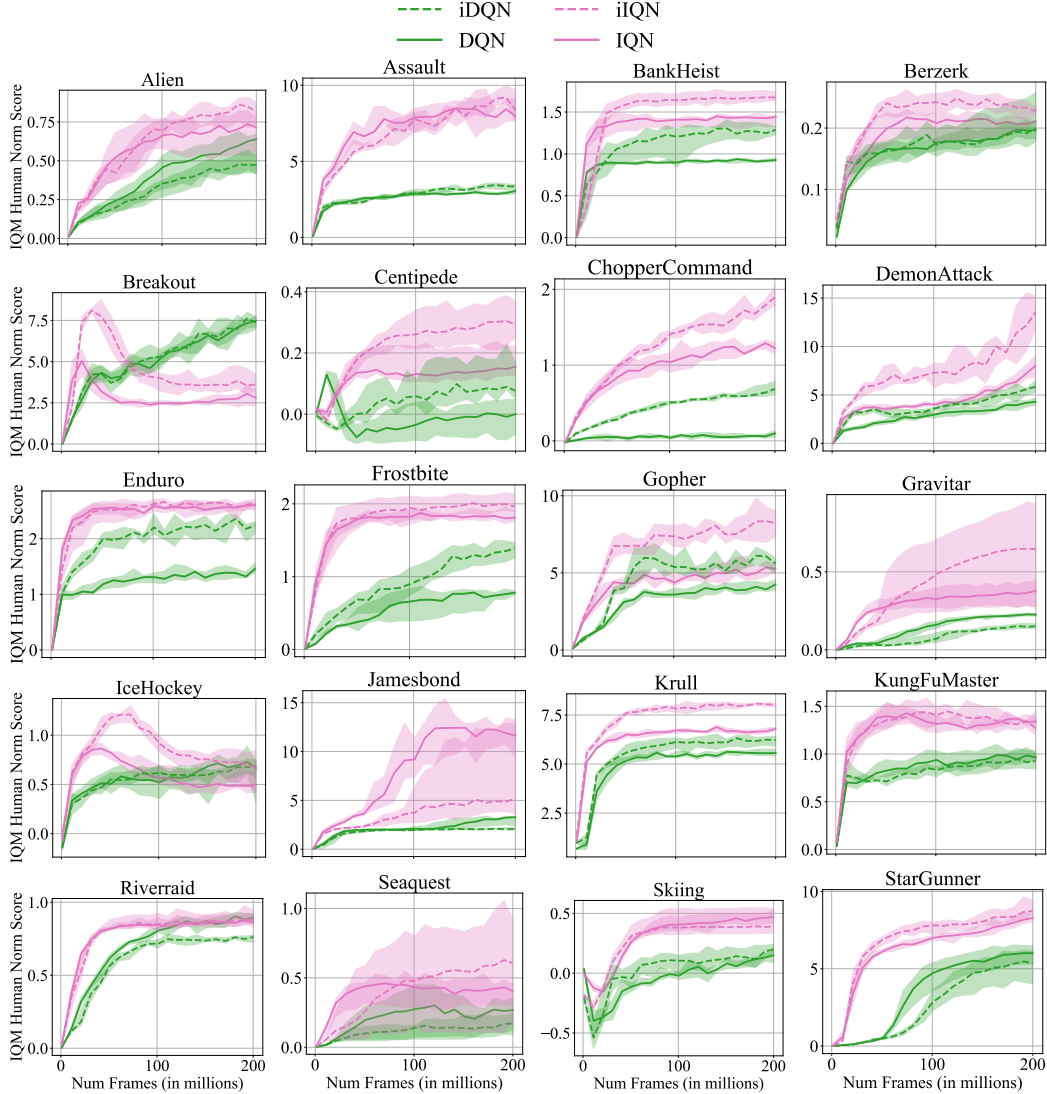


Figure 17: Training curves of iDQN with $K = 5$, iDQN + 3-step with $K = 5$ and iIQN with $K = 3$ along with DQN, Rainbow and iIQN on 20 Atari games. As a reminder, IQN is also using a 3-step return. In most games, the iterated approach outperforms its respective sequential approach.

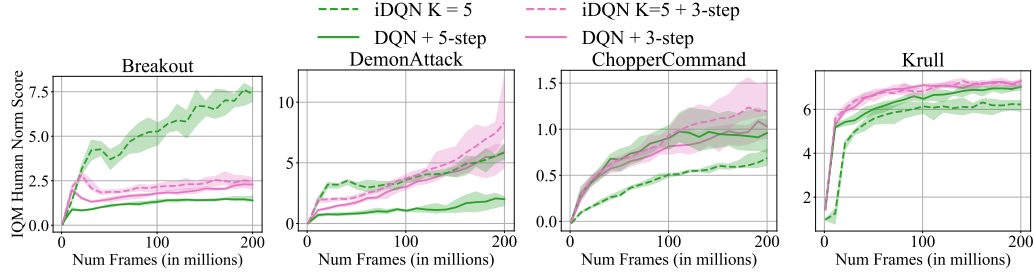


Figure 18: iDQN with $K = 5$ behaves differently than DQN + 5-step return. DQN + 3-step return is boosted by combining it with iDQN with $K = 5$.

Independent networks yield better scores compared to layer sharing, albeit at increased computational cost. In Figure 19, we show the performance of iDQN when the convolution layers are shared and when the neural networks are independent from each other on 2 Atari games. In *ChopperCommand*, having fully independent networks seems to be more beneficial than sharing the convolutional layers. We conjecture that this is due to the fact that the Bellman updates are far away from each other, hence the difficulty of representing consecutive Bellman updates with shared convolutional layers. Agarwal et al. (2020) share the same conclusion for Random Ensemble Mixture (REM) (Agarwal et al., 2020). They explain that independent networks are more likely to cover a wider space in the space of Q -functions. In *CrazyClimber*, both algorithms converge to the same score.

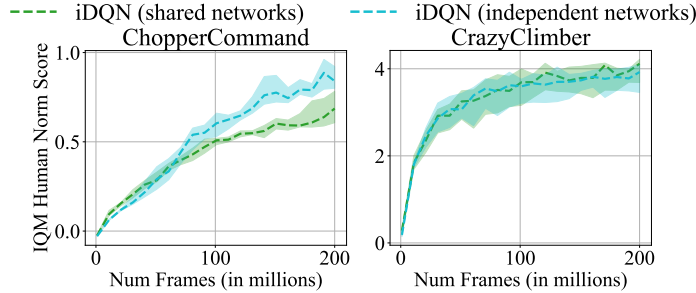


Figure 19: Independent networks can yield better performances than networks with shared convolutions.

Learned Q -functions demonstrate variability during training, coming closer to each other at the end of training. iDQN heavily relies on the fact that the learned Q functions are located within different areas in the space of Q -functions. To verify this assumption, we computed the standard deviation of the output of the learned Q -functions during the training in Figure 20. This figure shows that the standard deviation among the Q -function is indeed greater than zero across the 3 studied games. Furthermore, the standard deviation decreases during training, suggesting they become increasingly closer. This matches the intuition that at the end of the training, the iteration of the Q -functions should lie at the boundary of the space of the space of representable Q -functions, close to each other.

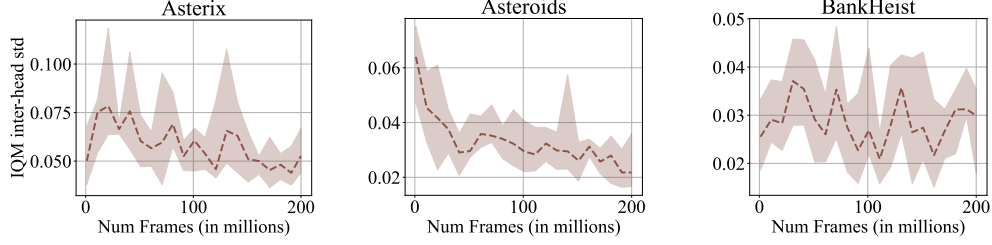


Figure 20: Standard deviation of the output of the 5 online networks of iDQN averaged over 3200 samples at each iteration. The standard deviation is greater than zero, indicating that the online networks are different from each other. The signal has a tendency to decrease, which matches our intuition that the Q -functions become increasingly close to each other as they get closer to the optimal Q -function.

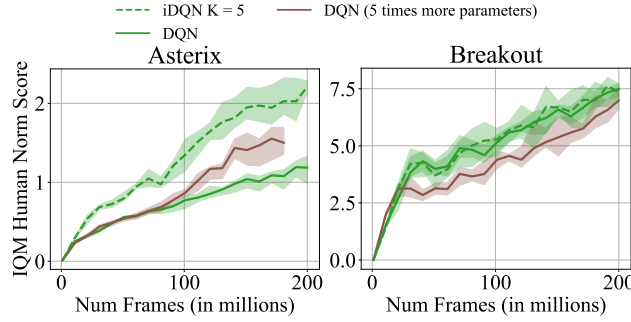


Figure 21: Inflating the number of parameters of DQN until it reaches the memory needed to run iDQN with $K = 5$ does not lead to performances as high as iDQN on the 2 considered games. Notably, while iDQN uses the same architecture as DQN, the inflated version of DQN uses a larger architecture than DQN.

F Training curves for MuJoCo control problems

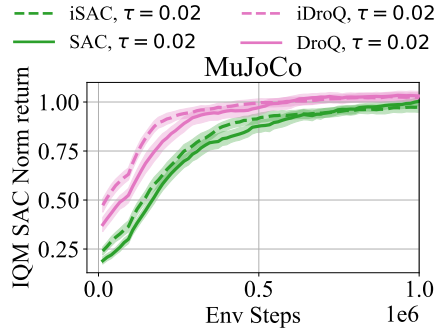


Figure 22: The iterated versions of SAC and DroQ with $K = 4$ also outperform their sequential versions when all the hyperparameters are the same.

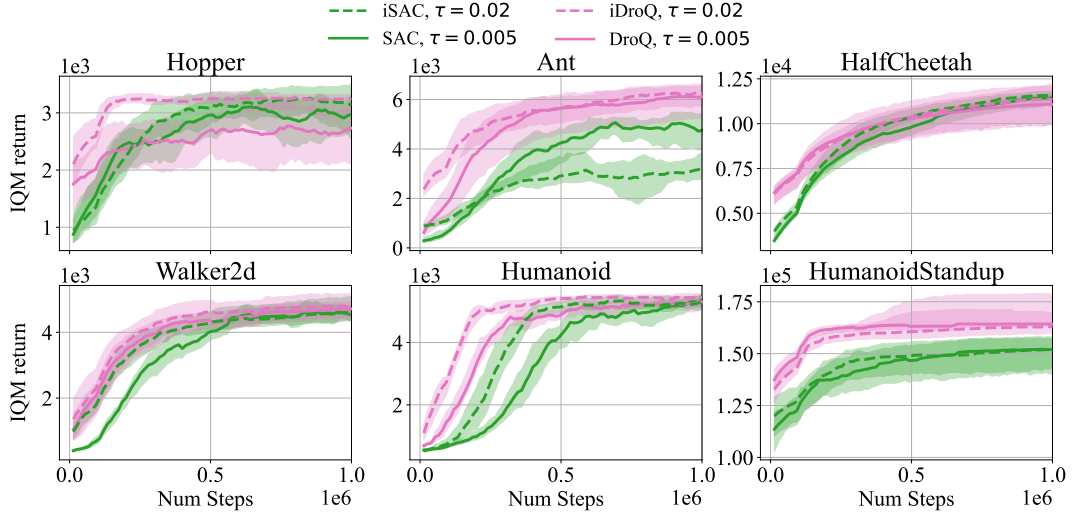


Figure 23: Training curves of iSAC with $K = 4$, iDroQ with $K = 4$ along with SAC and DroQ on 6 MuJoCo environments. In most problems, the iterated approach outperforms the sequential approach.

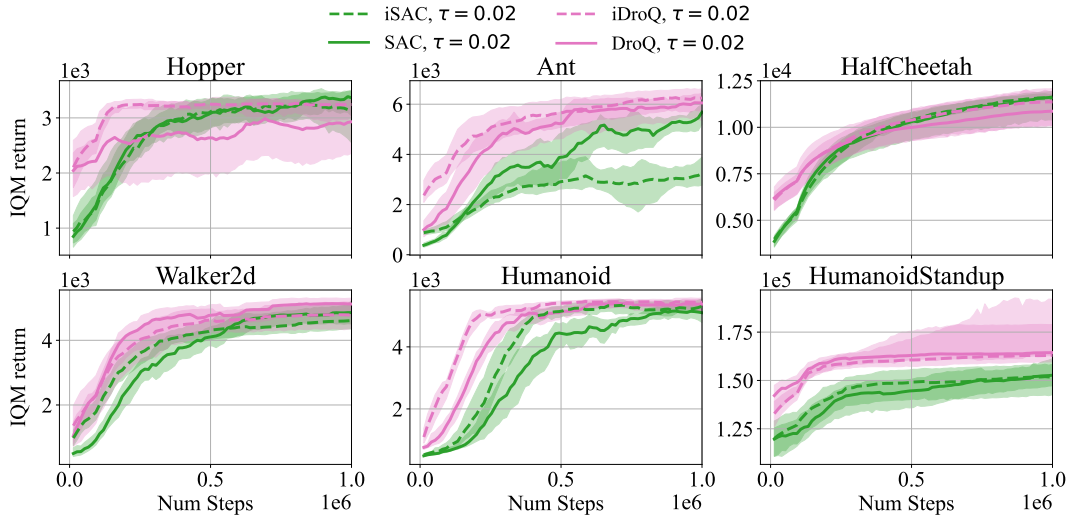


Figure 24: Training curves of iSAC with $K = 4$, iDroQ with $K = 4$ along with SAC and DroQ on 6 MuJoCo environments. In most problems, the iterated approach outperforms the sequential approach.